

# No-Drag String Configurations for Steadily Moving Quark-Antiquark Pairs in a Thermal Bath

Philip C. Argyres, Mohammad Edalati,  
and J.F. Vázquez-Poritz

*Physics Dept., Univ. of Cincinnati, Cincinnati OH 45221-0011*

argyres, edalati, jporitz@physics.uc.edu

## Abstract

We investigate the behavior of stationary string configurations on a five-dimensional AdS black hole background which correspond to quark-antiquark pairs steadily moving in an  $\mathcal{N} = 4$  super Yang-Mills thermal bath. There are many branches of solutions, depending on the quark velocity and separation as well as on whether Euclidean or Lorentzian configurations are examined.

# 1 Introduction and summary

The AdS/CFT correspondence provides a powerful tool with which to study the strong-coupling behavior of certain non-Abelian gauge theories in terms of semi-classical supergravity descriptions [1–4]. The most-studied example is four-dimensional  $\mathcal{N} = 4$   $SU(N)$  supersymmetric Yang-Mills theory (SYM) which, in the limit of large  $N$  and large 't Hooft coupling, is described by type IIB supergravity on  $AdS_5 \times S^5$ . Since at finite temperature the superconformal invariance of this theory is broken, and since fundamental matter can be added by introducing D7-branes [5], it is thought that this model may shed light on certain aspects of strongly-coupled QCD plasmas. For example, for any strongly-coupled large  $N$  gauge theory with a gravity dual, the dimensionless ratio of the shear viscosity over entropy density has been found to be  $1/4\pi$  [6–9] in rough agreement with some hydrodynamic models of RHIC collisions [10, 11].

More generally, the RHIC experiment has raised the issue of how to calculate the transport properties of relativistic partons in a hot, strongly-coupled gauge theory plasma. For example, one would like to calculate the friction coefficient and jet quenching parameter which are measures of the rate at which partons lose energy to the surrounding plasma [12–15]. Using conventional quantum field theoretic tools one can calculate these parameters only when the partons are interacting perturbatively with the surrounding plasma. The AdS/CFT correspondence may be a suitable framework in which to study strongly-coupled QCD-like plasmas. In fact, attempts to use the AdS/CFT correspondence to calculate these quantities have been made in [16–20] and were generalized in various ways in [21–37].

Finite-temperature  $\mathcal{N} = 4$   $SU(N)$  SYM theory is equivalent to the near-horizon limit of type IIB supergravity on the background of a large number  $N$  of non-extremal D3-branes stacked at a point. From the perspective of five-dimensional gauged supergravity, this is the background of an AdS black hole whose Hawking temperature equals the temperature of the gauge theory. According to the AdS/CFT dictionary, string configurations on this background can correspond to quarks and antiquarks in an  $\mathcal{N} = 4$  SYM thermal bath [38–41], where the quark bare mass is determined by the radial location of the string endpoints on a probe D7-brane.

A stationary single quark can be described by a string that stretches from the probe D7-brane to the black hole horizon. The semi-infinite string solution with a tail which drags behind a steadily moving endpoint and asymptot-

ically approaches the horizon has been proposed [17–19] as the configuration dual to a steadily moving quark in the  $\mathcal{N} = 4$  plasma, and was used to calculate the drag force on the quark.

A stationary quark-antiquark pair or “meson”, on the other hand, corresponds to a string with both endpoints ending on the D7-brane [5, 38, 39]. A class of such solutions, namely smooth, static solutions ( $v = 0$ ), have been used to calculate the inter-quark potential in SYM plasmas. Smooth, stationary solutions ( $v \neq 0$ ) for steadily moving quark pairs exist [34, 35, 37, 42, 43] but are not unique and do not “drag” behind the string endpoints as in the single quark configuration. This lack of drag has been interpreted to mean that color-singlet mesons are invisible to the SYM plasma and so experience no drag (to leading order in large  $N$ ) although the string shape is dependent on the velocity of the meson with respect to the plasma. (These timelike Lorentzian string solutions are reviewed in section 3, below.)

On the other hand, a prescription for computing the jet quenching parameter  $\hat{q}$  using the lightlike limit of spacelike Lorentzian configurations has been proposed in [16].<sup>1</sup> In this paper, we restrict ourselves to timelike Lorentzian and Euclidean configurations, and address spacelike Lorentzian configurations in [44].

**Summary.** Concretely, we consider a smooth stationary string in the background of an AdS<sub>5</sub> black hole with metric

$$ds_5^2 = h_{\mu\nu} dx^\mu dx^\nu = \eta \frac{r^4 - r_0^4}{r^2 R^2} dx_0^2 + \frac{r^2}{R^2} (dx_1^2 + dx_2^2 + dx_3^2) + \frac{r^2 R^2}{r^4 - r_0^4} dr^2. \quad (1.1)$$

$R$  is the curvature radius of the AdS space, and the black hole horizon is located at  $r = r_0$ . Since we are interested in (timelike) Lorentzian as well as Euclidean configurations, we have introduced the factor  $\eta$ ; for Lorentzian signature  $\eta = -1$  while for Euclidean signature it equals  $+1$ .

We put the endpoints of the string on a probe D7-brane at radius  $r_7$ .<sup>2</sup> The classical dynamics of the string in this background is described by the

---

<sup>1</sup>See footnote 14 of [34]. We thank H. Liu, K. Rajagopal, and U. Wiedemann for correspondence clarifying this point.

<sup>2</sup>The background (1.1) can be lifted to ten dimensions on a 5-sphere, where it is the near-horizon geometry of a stack of  $N$  non-extremal D3-branes. The probe D7-brane wraps an  $S^3$  inside the  $S^5$  and fills the entire AdS<sub>5</sub> background down to a minimal radius  $r_7$  [5, 45–49]. We assume no motion on the  $S^5$ , and so use the five-dimensional perspective.

Nambu-Goto action

$$S = \frac{\eta}{2\pi\alpha'} \int d\sigma d\tau \sqrt{\eta G}, \quad (1.2)$$

where  $G = \det(G_{\alpha\beta})$ ,  $G_{\alpha\beta} = h_{\mu\nu} \partial_\alpha X^\mu \partial_\beta X^\nu$  is the induced metric on the string worldsheet, and  $\partial_\alpha := \partial/\partial\xi^\alpha$ , with  $\xi^\alpha = \{\tau, \sigma\}$  being the worldsheet coordinates. Here  $X^\mu$  run over the five coordinates  $\{x_0, x_1, x_2, x_3, r\}$ .

The steady state of a quark-antiquark pair with constant separation and moving with constant velocity either perpendicular or parallel to the separation of the quarks can be described (up to worldsheet reparameterizations) by the worldsheet embedding

$$\begin{aligned} [v_\perp] : \quad & x_0 = \tau, \quad x_1 = v\tau, \quad x_2 = \sigma, \quad x_3 = 0, \quad r = r(\sigma), \\ [v_\parallel] : \quad & x_0 = \tau, \quad x_1 = v\tau + \sigma, \quad x_2 = 0, \quad x_3 = 0, \quad r = r(\sigma), \end{aligned} \quad (1.3)$$

where the first is for the velocity perpendicular to the quark separation, and the second parallel to it. In both cases we take boundary conditions

$$0 \leq \tau \leq T, \quad -\frac{L}{2} \leq \sigma \leq \frac{L}{2}, \quad r(\pm L/2) = r_\tau, \quad (1.4)$$

with  $r(\sigma)$  smooth.<sup>3</sup>

In section 2 we derive the equations of motion describing configurations corresponding to quark-antiquark pairs, in both Lorentzian as well as Euclidean signature, which are stationary and smooth. As argued in [35], smooth string configurations cannot drag behind their endpoints as they dip down from the D7-brane. Among these no-drag configurations, we concentrate on two simple geometries, where the common velocity of the quark pair is either perpendicular or parallel to their separation.

We examine the timelike Lorentzian solutions of these equations in some detail in section 3. In the case that the meson velocity is perpendicular to the quark separation  $L$ , we review the known solutions. Up to a maximum  $L \leq L_c(v)$  which decreases with increasing velocity, there are two branches of Lorentzian solutions: one “long” whose radial turning point is closer to

---

<sup>3</sup>The endpoints of a string on a D-brane satisfy Neumann boundary conditions in the directions along the D-brane, whereas the above boundary conditions are Dirichlet, constraining the string endpoints to lie along fixed worldlines a distance  $L$  apart on the D7-brane. The correct way to impose these boundary conditions is to turn on a worldvolume background  $U(1)$  field strength on the D7-brane [17] to keep the string endpoints a distance  $L$  apart.

the horizon than the “short” solution. For  $L > L_c(v)$ , quark-antiquark pairs only exist as free states described by two disconnected strings. These two branches, as well as the complete screening length, have been discussed in [34, 35, 37, 42, 43]. The long string solution which makes it closer to the horizon has been argued to be unstable [35, 43] and presumably decays into the shorter string configuration which shares the same boundary conditions. This is supported by the fact, shown in section 4, that the energy of the Euclideanized version of the long string configuration is greater than that of the short string.

When the meson velocity is parallel to the quark separation, the long string configurations are not smooth, but instead develop a cusp at the midpoint for a range of velocities. The tip of the cusp is lightlike. On the other hand, the short string solution is always smooth.

In section 4 we examine the Euclidean string configurations in detail. Their main interest lies in the fact that their relative thermodynamic stability can be determined by comparing their actions (energies). However, we find that not all Euclidean solutions have Lorentzian counterparts.

Euclidean configurations for which the velocity is parallel to their separation share some of the same characteristics as the timelike Lorentzian configurations. Namely, there tend to be two different branches of solutions, except when  $v > 1$ , for which there is only one. (There is no restriction to  $v < 1$  for Euclidean strings;  $v$  is more properly thought of as a slope parameter, rather than a velocity.) Also, there is a maximum distance between the quark and the antiquark past which only free quarks exist.

On the other hand, for Euclidean configurations with velocity perpendicular to their separation, the discussion of the various branches of string solutions becomes more involved. Firstly, some of the branches no longer have a maximum value of  $L$ . Secondly, the number of branches now depends on the velocity. In particular, for low velocities there are actually four branches of solutions, while only two branches exist for higher velocities. The solutions in which the string dips closer to the black hole horizon are less energetically favorable.

## 2 Equations of motion

According to the AdS/CFT correspondence [4] strings ending on the D7-brane are equivalent to quarks in a thermal bath in four-dimensional finite-

temperature  $\mathcal{N}=4$   $SU(N)$  super Yang-Mills (SYM) theory. The standard gauge/gravity dictionary is that

$$N = R^4/(4\pi\alpha'^2 g_s), \quad \lambda = R^4/\alpha'^2, \quad \beta = \pi R^2/r_0, \quad m = r_7/(2\pi\alpha'), \quad (2.1)$$

where  $g_s$  is the string coupling,  $\lambda := g_{\text{YM}}^2 N$  is the 't Hooft coupling of the SYM theory,  $\beta$  the inverse temperature of the SYM thermal bath, and  $m$  the quark mass at zero temperature. In the semiclassical string limit, *i.e.*,  $g_s \rightarrow 0$  and  $N \rightarrow \infty$ , the supergravity approximation in the gauge/gravity correspondence holds when the curvatures are much greater than the string length,  $\ell_s := \sqrt{\alpha'}$ . Furthermore, in this limit the mass of the quark is identified with the energy (in some units) of the associated string which, for a static configuration, is just proportional to the value of the Nambu-Goto action (1.2).

Now, the string embeddings (1.3) considered here (and elsewhere) depend on three additional parameters:  $T$ ,  $L$ , and  $v$ . According to the standard AdS/CFT dictionary, these are the time for which the quarks are propagating, their separation at a given time, and their common velocity, respectively—all in the plasma rest frame. Also, it is easy to see from (1.1) and (1.3) that, for Lorentzian ( $\eta = -1$ ) solutions, the proper velocity  $V$  of the string endpoints on the  $r = r_7$  surface in the AdS black hole background is related to the velocity  $v$  in the four-dimensional field theory by

$$V = \frac{r_7^2}{\sqrt{r_7^4 - r_0^4}} v. \quad (2.2)$$

Note that real string solutions must have the same signature everywhere on the worldsheet. Thus, a string worldsheet will be timelike or spacelike depending on whether  $V$ , rather than  $v$ , is greater or less than 1. In particular, the string worldsheet is timelike for  $V < 1$  which in terms of  $v$  translates into  $v < \sqrt{1 - (r_0/r_7)^4}$ . (In Euclidean signature,  $v$  is more properly thought of as an angular parameter, and  $V$  is likewise a proper version of this parameter as measured in the Euclidean AdS black hole metric. This will be discussed more in section 4.2.)

With the embeddings (1.3) and boundary conditions (1.4), the action

becomes

$$\begin{aligned}
[v_{\perp}] : \quad S &= \frac{\eta T}{\gamma \pi \alpha'} \int_0^{L/2} d\sigma \sqrt{\frac{r^4 - \gamma^2 r_0^4}{R^4} + \frac{r^4 - \gamma^2 r_0^4}{r^4 - r_0^4} r'^2}, \\
[v_{\parallel}] : \quad S &= \frac{\eta T}{\gamma \pi \alpha'} \int_0^{L/2} d\sigma \sqrt{\gamma^2 \frac{r^4 - r_0^4}{R^4} + \frac{r^4 - \gamma^2 r_0^4}{r^4 - r_0^4} r'^2}, \tag{2.3}
\end{aligned}$$

where  $r' := \partial r / \partial \sigma$  and

$$\gamma^2 := \frac{1}{1 + \eta v^2}. \tag{2.4}$$

Thus,  $\gamma$  is the usual relativistic  $\gamma$ -factor for Lorentzian signature ( $\eta = -1$ ), while it is always a positive number less than 1 for Euclidean signature ( $\eta = +1$ ).

We find for the equations of motion

$$\begin{aligned}
[v_{\perp}] : \quad r'^2 &= \frac{1}{\gamma^2 a^2 r_0^4 R^4} (r^4 - r_0^4) (r^4 - \gamma^2 [1 + a^2] r_0^4), \\
[v_{\parallel}] : \quad r'^2 &= \frac{\gamma^2}{a^2 r_0^4 R^4} (r^4 - r_0^4)^2 \frac{(r^4 - [1 + a^2] r_0^4)}{(r^4 - \gamma^2 r_0^4)}, \tag{2.5}
\end{aligned}$$

where  $a^2$  is a real integration constant. Although we have written  $a^2$  as a square, it can be either positive or negative. Using (2.5), the determinant of the induced worldsheet metric becomes

$$\begin{aligned}
[v_{\perp}] : \quad G &= \eta \frac{1}{\gamma^4 a^2 r_0^4 R^4} (r^4 - \gamma^2 r_0^4)^2, \\
[v_{\parallel}] : \quad G &= \eta \frac{1}{a^2 r_0^4 R^4} (r^4 - r_0^4)^2. \tag{2.6}
\end{aligned}$$

Thus, the sign of  $G$  is the same as that of  $\eta a^2$  (since the other factors are squares of real quantities). In particular, for Euclidean signature ( $\eta = +1$ ) all real worldsheets have  $G > 0$ , and so we must take  $a^2 > 0$ . For Lorentzian signature ( $\eta = -1$ ), the worldsheet is timelike ( $G < 0$ ) for  $a^2 > 0$  and spacelike for  $a^2 < 0$ .

The reality of  $r'$  implies that the right sides of (2.5) must be positive in all these different cases. This positivity then implies certain allowed ranges of  $r$ . There can only be real string solutions when the ends of the string, at  $r = r_7$ , are within this range. The edges of this range are (typically) the possible

turning points,  $r_t$ , for the string. We will describe the possible values of  $r_t$  for the timelike Lorentzian and Euclidean cases in the following sections.

Given these turning points, (2.5) can be integrated for a string solution which goes from  $z_7$  to the turning point  $z_t$  and back to give

$$\begin{aligned}
[v_\perp] : \quad L/\beta &= \frac{2a\gamma}{\pi} \int_{z_t}^{z_7} \frac{dz}{\sqrt{(z^4 - 1)(z^4 - (1 + a^2)\gamma^2)}}, \\
[v_\parallel] : \quad L/\beta &= \frac{2a}{\pi\gamma} \int_{z_t}^{z_7} \frac{dz \sqrt{z^4 - \gamma^2}}{(z^4 - 1)\sqrt{z^4 - (1 + a^2)}}, \tag{2.7}
\end{aligned}$$

where we have used  $r_0 = \pi R^2/\beta$ . Also, in (2.7) we have rescaled  $z = r/r_0$  and likewise  $z_t := r_t/r_0$  and  $z_7 := r_7/r_0$ . These integral expressions determine the integration constant  $a^2$  in terms of  $L/\beta$  and  $v$ .

Also, we can evaluate the action for the solutions of (2.5) to be:

$$\begin{aligned}
[v_\perp] : \quad S &= \frac{\eta T \sqrt{\lambda}}{\gamma\beta} \int_{z_t}^{z_7} \frac{(z^4 - \gamma^2) dz}{\sqrt{(z^4 - 1)(z^4 - \gamma^2[1 + a^2])}}, \\
[v_\parallel] : \quad S &= \frac{\eta T \sqrt{\lambda}}{\gamma\beta} \int_{z_t}^{z_7} dz \sqrt{\frac{z^4 - \gamma^2}{z^4 - [1 + a^2]}}, \tag{2.8}
\end{aligned}$$

where we have used  $R^2/\alpha' = \sqrt{\lambda}$ . For finite  $z_7$ , these integrals are convergent. They diverge when  $z_7 \rightarrow \infty$ , and need to be regularized by subtracting the self-energy of the quark and the antiquark [38, 39].

### 3 Timelike Lorentzian solutions

Turning now to timelike Lorentzian ( $\eta = -1$ ) string configurations, we see from (2.6) that the integration constant  $a^2$  must be positive. An analysis of (2.5), bearing in mind (2.2), easily shows that real solutions can exist only for  $v < \sqrt{1 - z_7^{-4}}$  and as long as the string is at radii satisfying

$$\begin{aligned}
[v_\perp] : \quad r^4/r_0^4 &> \gamma^2(1 + a^2), \\
[v_\parallel] : \quad r^4/r_0^4 &> \max \{ \gamma^2, 1 + a^2 \}. \tag{3.1}
\end{aligned}$$

We will first briefly review the case in which the velocity of the quark-antiquark pair is perpendicular to their separation [34, 35, 37] and then consider the parallel case.



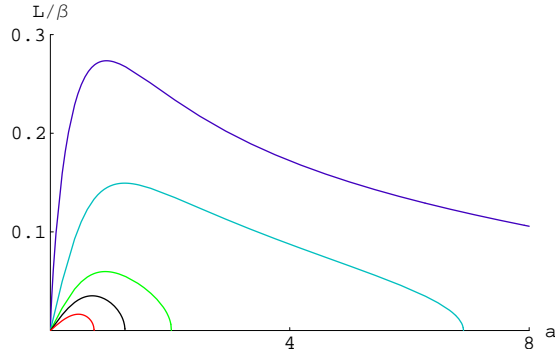


Figure 1:  $L/\beta$  as a function of  $a$  for timelike Lorentzian string configurations with velocity perpendicular to the quark separation,  $z_7 = 2$ , and  $\gamma = 1$  (dark blue), 1.5 (light blue), 2 (green), 3 (black), and 3.8 (red).

### 3.1 Timelike Lorentzian: perpendicular velocity

Equation (3.1) implies that the radial turning point of the string is at  $z^4 := (r/r_0)^4 = \gamma^2(1 + a^2)$ . It also implies that, for a given velocity parameter  $v$ , the minimum D7-brane radius  $z_7 := r_7/r_0$  reached by the probe must also be set to be greater than this value. ( $z_7$  should also be set greater than the critical value  $z_7^c \approx 1.02$ , below which the D7-brane dips into the horizon, changing the topology of the space [45–49].)

For a given choice of  $z_7$ , (2.7) can be numerically integrated to give  $L/\beta$  as a function of  $a$ , as shown in figure 1 for a few sample velocities with the choice  $z_7 = 2$ . (A similar plot has already been presented in [35].) The qualitative features of the plots are not sensitive to the particular value of  $z_7$ , though one should bear in mind that the range of allowed velocity parameters  $v$  depends on  $z_7$ , since the string endpoints become spacelike for  $\gamma > z_7^2$ , as can be seen from (2.2).

Figure 1 illustrates the fact that, for each value of  $L$  that is less than a critical value  $L_c(v)$ , there are two corresponding values of  $a$ , and  $L_c(v)$  decreases with increased velocity  $v$ . We shall refer to the branch of string configurations with smaller (larger)  $a$  for a given  $L$  as the long (short) configurations. For  $L > L_c$  there is no connected string solution:  $L_c$  corresponds to a complete screening length past which quarks and antiquarks only exist as free states [30, 34, 35, 37].

We have plotted in figure 2 both long and short string configurations for fixed  $L/\beta$  and various velocities. The radial direction is horizontal, the  $x_2$ -

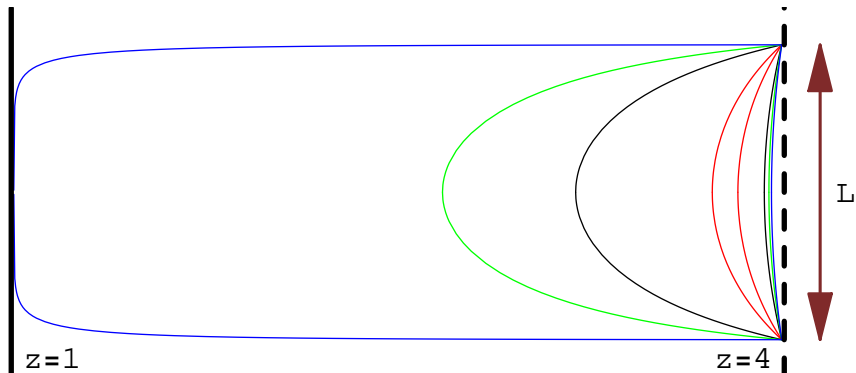


Figure 2: Timelike Lorentzian string configurations with velocity perpendicular to the quark separation,  $L/\beta = 0.1$ , and  $\gamma = 1$  (blue), 1.5 (green), 2 (black), and 2.1 (red). For each velocity there are two string solutions, one long and one short. The black hole horizon (solid black line) is at  $z = 1$  and the minimal radius reached by the probe D7-brane (dotted line) is at  $z = z_7 = 2$ .

direction is vertical and the velocity is orthogonal to both. The black hole horizon is represented by the solid black line at  $z = 1$  and the probe D7-brane corresponds to the dashed line at  $z = z_7$ . For zero velocity (blue curves), the long string configuration almost touches the black hole horizon. As the velocity is increased so the string worldsheets become more nearly lightlike ( $V \rightarrow 1$ , or  $\gamma \rightarrow 4$ ), the long and short string configurations shorten and lengthen, respectively, and approach a common limiting shape (between the red curves). They coincide when the velocity reaches some  $\gamma = \gamma_c$  ( $\gamma_c \approx 2.112$  for the specific values of  $L/\beta$  and  $z_7$  in the figure). This is the value of the velocity parameter where  $L_c = L$ ; for greater velocities there are no string solutions for this given  $L$  and  $z_7$ . A general qualitative property of these solutions is that for any fixed  $L$  and  $z_7$  there is no lightlike limit of these timelike string configurations: the limiting  $L = L_c$  is reached before  $V = 1$ .

We will see in section 4 that the Euclidean counterparts of the long string solutions are not energetically favored. This indicates that this branch of solutions is not stable: a long string state presumably decays into the corresponding short string which has the same boundary conditions. The instability of the long string configurations was hypothesized in [35] and has been argued for dynamically in [43].

## 3.2 Timelike Lorentzian: parallel velocity

We will now look at the situation for which the velocity is in the same direction as the quark-antiquark separation. Recall that reality of  $r'$  and the equation of motion (2.5) implied (3.1); that is, the allowed region is  $z^4 > \max\{\gamma^2, 1 + a^2\}$ . Unlike the perpendicular case, this boundary is not always a smooth turning point of the string. In particular, (2.5) implies that  $r' = 0$  when  $z = 1 + a^2$ , which is a smooth turning point (the string reaches a minimum); but  $r' = \infty$  when  $z^4 = \gamma^2$ . This latter behavior signals the development of a cusp at the string midpoint. As we discussed in section 2,  $z^4 = \gamma^2$  is also the place where the string worldsheet changes from timelike to spacelike signature. Since, by (2.6), real string solutions cannot change their worldsheet signature, we conclude that whenever  $\gamma^2 > 1 + a^2$  this cusp is unavoidable.<sup>4</sup>

It is not obvious when  $\gamma^2 > 1 + a^2$  is satisfied, since  $a^2$  is determined in terms of  $v$  through (2.7). In figure 3 we integrate (2.7) for various velocities to give an indication of how  $a$  depends on  $L$  and  $v$ . Figure 3 actually shows the quark separation  $L_0 := \gamma L$  in the quark rest frame rather than the separation  $L$  in the plasma restframe. There are two branches of solutions for  $a$  when  $L_0 < L_{0c}(v)$ , none when  $L_0 > L_{0c}(v)$ , and  $L_{0c}(v)$  decreases for increasing  $v$ . This is qualitatively similar to the perpendicular velocity case.

The shaded region in figure 3 is for  $\gamma^2 > 1 + a^2$ , in which case the string solutions have a cusp. Note that this region lies to the left of the maximum of the constant- $v$  curves in the figure. This means that the large- $a$  (short string) solutions never have cusps but that, depending on the values of  $L_0$  and  $v$ , the long string solutions may. Typically, for given  $L_0$  the long string solutions for small enough  $v$  (close to  $v = 0$ ) and large enough  $v$  (near where  $L_{0c}(v)$  approaches  $L_0$ ) are smooth, while at intermediate  $v$  there are cusps.

---

<sup>4</sup> Without this physical argument, one might imagine that the  $r' = \infty$  vertical tangent is a signal not of a cusp, but just that the string solution should be extended to include a smooth but self-intersecting closed loop. The worldsheet embedding (1.3) we have used does not allow for this extension, and so one might think that the cusp could be avoided by using a different embedding. For example, instead of using a parameterization in which  $x_1 = v\tau + \sigma$  as in (1.3), which forces the string to vary monotonically in the  $x_1$  direction, one might use a different parameterization with, say,  $r = \sigma$  and  $x_1 = v\tau + x(\sigma)$  for some undetermined function  $x(\sigma)$ . This would, in principle, allow the string to cross itself and form a smooth loop. However, reworking our calculations in this alternative parametrization gives equations of motion completely equivalent to (2.5). Thus, this possibility is not realized, and the cusps cannot be avoided, in agreement with the physical argument.

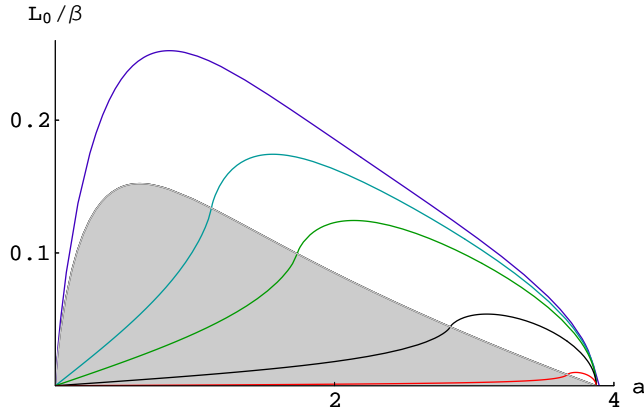


Figure 3:  $L_0/\beta$  as a function of  $a$  for a timelike Lorentzian string with velocity parallel to quark separation,  $z_7 = 2$ , and  $\gamma = 1$  (dark blue), 1.5 (light blue), 2 (green), 3 (black), and 3.8 (red). Strings corresponding to points in the shaded region have cusps.

This is illustrated for  $z_7 = 2$  and  $L_0/\beta = 0.1$  in figure 4. There the  $\gamma = 0$  (blue) and  $\gamma = 2.5$  (red) long strings have no cusp, while the intermediate velocity (green and black) strings do.<sup>5</sup> Just as in the case of perpendicular velocity, as  $v$  is increased the long and short strings approach one another until they coincide at a critical value of the velocity parameter ( $\gamma \approx 2.6173$  for the values of the parameters in the figure), beyond which there are no more connected solutions. Note that this critical velocity parameter is short of the lightlike worldsheet limit  $\gamma = z_7^2$  so that, as in the case of perpendicular velocity, no lightlike worldsheet limit of the connected timelike configuration exists at fixed  $L_0$  and  $z_7$ .

## 4 Euclidean strings and their energetics

Real Euclidean ( $\eta = +1$ ) string configurations must have positive integration constant  $a^2$ , by (2.6). An analysis of (2.5) easily shows that real solutions can exist for any  $v$  (since now  $1 \geq \gamma > 0$  for all  $v$ ) as long as the string is at

---

<sup>5</sup>The appearance of a kink—for which there is a finite opening angle—rather than a cusp in the green and black long strings in figure 4 is misleading: the cusp behavior is apparent with sufficient resolution.

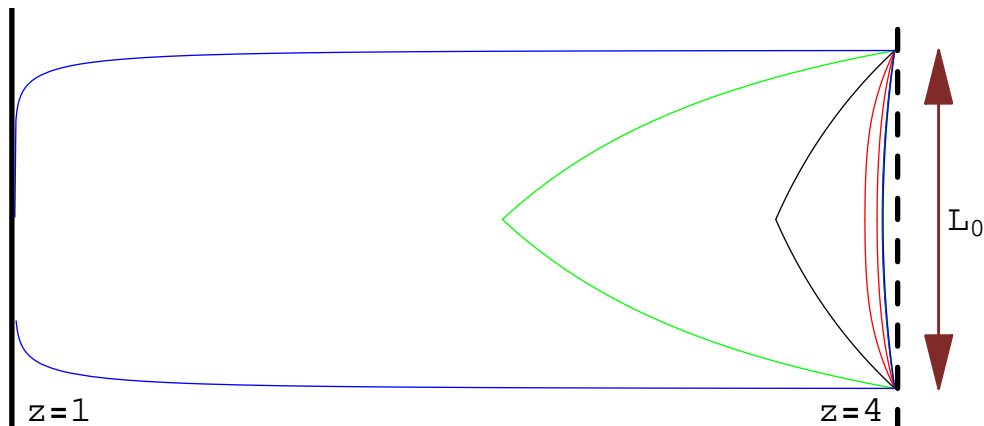


Figure 4: Timelike Lorentzian configurations with velocity parallel to quark separation,  $L_0/\beta = 0.1$ , and  $\gamma = 1$  (blue), 1.5 (green), 2 (black) and 2.5 (red).

radii satisfying

$$\begin{aligned}
 [v_{\perp}] : \quad & r^4/r_0^4 > \max \{1, \gamma^2(1+a^2)\}, \\
 [v_{\parallel}] : \quad & r^4/r_0^4 > 1+a^2.
 \end{aligned} \tag{4.1}$$

Nothing special happens in Euclidean signature as the “velocity” parameter  $v \rightarrow 1$ . Indeed,  $v$  is more properly thought of as an angular parameter in Euclidean space, though we will still refer to it as the velocity parameter.

Note that there are Euclidean solutions which are not Wick rotations of Lorentzian ones. Lorentzian and Euclidean equations of motion (2.5) are related to each other simply by taking  $v^2 \rightarrow -v^2$ . However, this does not mean that the corresponding solutions are simply related by Wick rotations since, under  $v^2 \rightarrow -v^2$ , the behavior of the turning points can change qualitatively. In particular, timelike Lorentzian solutions with perpendicular velocity always have  $r_t^4 = \gamma^2(1+a^2)r_0^4 > r_0^4$  and so the string never reaches the horizon. On the other hand, for  $a < v$  there is a branch of Euclidean solutions which have the radial turning point on the black hole horizon  $r = r_0$ . This branch of solutions has no physical Lorentzian counterpart. Other examples of Euclidean string configurations with no physical Lorentzian counterpart are easy to come by. For instance, the Wick rotation of a steadily moving, purely radial Euclidean string stretched between a probe D7-brane and the black hole horizon fails to exist in Lorentzian signature, since there is an intermediate radial point below which the string travels faster than the speed of light.

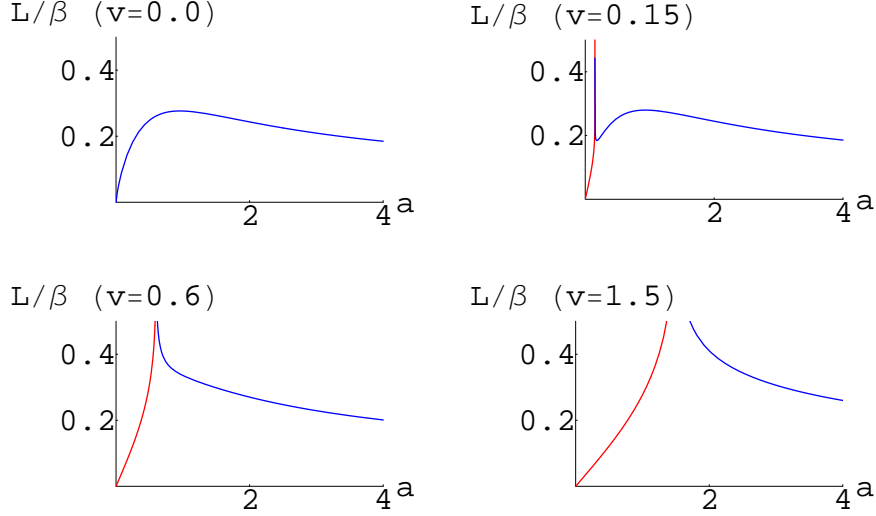


Figure 5:  $L/\beta$  as a function of  $a$  with  $z_7 = 2$  for Euclidean configurations with  $v = 0, 0.25, 0.5$  and  $1$ , for which the velocity is perpendicular to the quark separation. The red and blue curves represent solutions with  $a < v$  and  $a > v$ , respectively.

#### 4.1 Euclidean: perpendicular “velocity”

A numerical plot of  $L/\beta$  as a function of  $a$  for various velocities is shown in figure 5. We have set  $z_7 = 2$  as an example, though the plot is qualitatively unchanged for other values of this parameter. Since Wick rotation amounts to changing the sign of  $v^2$  in the equations, the configuration with  $v = 0$  is exactly the same for Lorentzian and Euclidean signatures. In particular, there are no solutions for  $L > L_c$ , and for a given value of  $L < L_c$  there are two string configurations. For  $v > 0$ , however, the story changes dramatically. Firstly, there is no longer a maximum value of  $L$ . Secondly, the number of branches of solutions depends on  $L$  as well as the velocity. For intermediate velocities, two new branches of configurations emerge which have no Lorentzian counterparts. This is shown in the upper right region of figure 5 for  $v = 0.25$ . One new branch, which is denoted by the red curve, has  $a < v$  and exists for all values of  $L/\beta$ . For small and large values of  $L/\beta$ , there is only one branch of blue solutions but for intermediate values of  $L/\beta$  there are actually three branches. For sufficiently large  $v$ , only one branch of blue solutions occurs. This is illustrated in the lower left region of figure 5 for

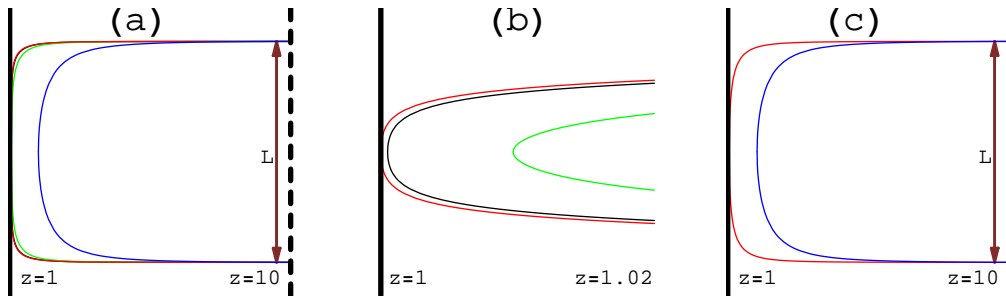


Figure 6: Euclidean string configurations with perpendicular velocity,  $L/\beta = 0.25$  and  $z_7 = 2$ . (a): Four solutions when  $v = 0.25$ , with  $a$  values of approximately 0.237 (red), 0.290 (black), 0.423 (green) and 1.172 (blue). (b): Two solutions when  $v = 0.5$  with  $a$  values approximately 0.397 (red) and 1.503 (blue).

$v = 0.5$ . For larger values of  $v$  there are no qualitative changes, as illustrated in the lower right of figure 5 for  $v = 1$ . (Nothing special happens at  $v = 1$  in Euclidean signature.)

To better illustrate this, the four different string configurations for  $v = 0.25$  and  $L/\beta = 0.25$  are plotted in figure 6(a). Only the  $a < v$  configuration, represented by the red curve, actually touches the black hole horizon. Only two of the branches of configurations remain for all  $L/\beta$  as the velocity is further increased, as illustrated in figure 6(b) for  $v = 0.5$ .

Which of these states is the physical one for a given set of parameters can be determined by comparing their energies. The intuition that the blue curve represents the energetically favorable solution, since it does not stretch as far towards the black hole, is born out by a calculation of the energies. The energy of the Euclidean string configurations is given by  $S/T$ , where  $S$  is the Nambu-Goto action given by (2.8) and  $T$  is the time interval.

It is more illuminating to discuss the energy difference  $E$  between these configurations and some standard string configuration. A simple and natural fiducial configuration to choose is that of two disconnected strings moving at “velocity”  $v$  which stretch from the probe D7-brane to the black hole horizon. So in our discussion below we will measure energies in comparison to these straight string configurations, which therefore have energy  $E = 0$  by definition.

$E\beta/\sqrt{\lambda}$  versus  $L/\beta$  is plotted in figure 7 for various velocities for the aforementioned configurations. The case of vanishing velocity has already been considered in [40, 41]. As before, the red curve represents the string

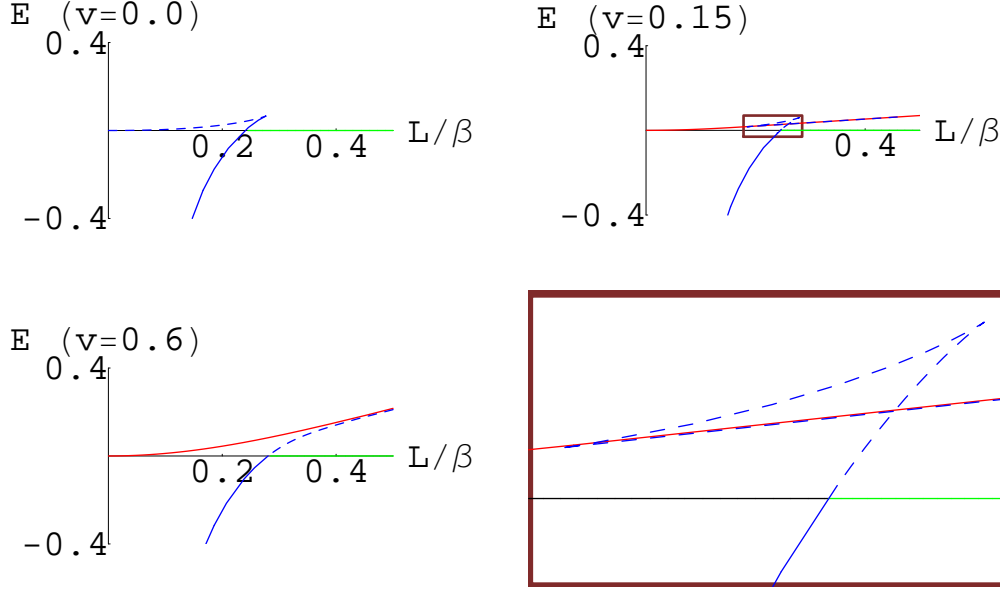


Figure 7: Energy in units of  $\sqrt{\lambda}/\beta$  versus  $L/\beta$  for Euclidean configurations with perpendicular velocity,  $z_7 = 2$ , and  $v = 0, 0.1$ , and  $0.5$ . The red and blue curves represent solutions with  $a < v$  and  $a > v$ , respectively, while the green line is the subtracted energy of two straight strings.

configuration with  $a < v$ , which reaches the black hole horizon. There are multiple configurations with  $a > v$  for a given  $L$  (blue curves), depending on the velocity. The energy of the fiducial straight string configuration is given by the  $E = 0$  line.

As can be seen from figure 7, for  $L$  less than a critical value, the energetically favorable state is represented by the blue curve. This is the string configuration that remains the furthest from the black hole horizon and is the Wick rotated counterpart of the timelike Lorentzian short string solution with perpendicular velocity that was discussed in section 3. As the distance between the quark and antiquark increases to the critical value, the subtracted energy of this configuration becomes positive. At this point, it is energetically favorable for the string to separate into two straight strings (green line). Note that the long string configuration (red curve) is always less energetically favorable than the short strings (blue curve), which agrees with the claim that the corresponding Lorentzian configurations are unsta-



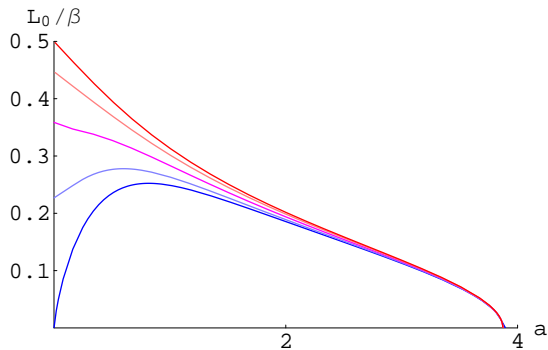


Figure 8:  $L_0/\beta$  as a function of  $a$  for Euclidean string configurations with parallel velocity,  $z_7 = 2$ , and  $v = 0$  (blue), 0.5 (light blue), 1 (purple), 2 (light red), and 5000 (red).

ble [35, 43].

It is tempting to identify the transition from the short string solution (blue) to the two straight string solution (green) as the transition in the field theory from a bound quark and antiquark pair to free quark pair due to complete screening by the thermal bath. However, this interpretation is problematical. The reason is that, as mentioned earlier, the straight Euclidean string is not the Euclidean rotation of any straight Lorentzian string solution (since at any nonzero  $v$  such a straight Lorentzian string becomes lightlike before it reaches the horizon, and so fails to exist as a solution). A physically acceptable Lorentzian free quark solution is the dragged string solution of [17, 18], so it may be more appropriate to compare the energy of the Euclidean short string solution (blue) to that of the Euclidean rotation of a pair of dragged strings instead. See [35] for a discussion of the issues involved in making this comparison. So the transition between the blue and green configurations illustrated in figure 8 gives at best an upper bound on the critical  $L$  at which complete screening by the SYM thermal bath occurs.

## 4.2 Euclidean: parallel “velocity”

For Euclidean string configurations with parallel “velocity”, (4.1) shows that the radial turning point is at  $r = (1 + a^2)^{1/4} r_0$ . Such solutions with  $V < 1$  are Wick rotations of the timelike Lorentzian solutions with corresponding

turning point (*e.g.*, all those outside of the shaded region in figure 3). In contrast to the configurations with perpendicular velocity, there is always a maximum  $L$  regardless of the magnitude of the velocity. Also, there are no string configurations that reach the black hole horizon.  $L_0/\beta$  versus  $a$  for various velocities is shown in figure 8. In Euclidean signature,  $L_0 := \gamma L$  measures the shortest distance between the “worldlines” of the endpoints of the strings. Since  $\arctan(V)$  measures the angle between these worldlines and the constant- $x_1$  planes, in the limit  $V \sim v \rightarrow \infty$  the worldlines coincide and  $L_0 \rightarrow 0$ . The curves in figure 8 ascend from  $v = 0$  to  $v = \infty$ . For  $V < 1$  there are two solutions for each value of  $L < L_c$ . The short string configurations correspond to the part of the curves to the right of the peak in figure 8, while the long configurations correspond to the left side. For  $V > 1$  there is only one solution and, as  $v \rightarrow \infty$ ,  $L_c/\beta \rightarrow \sqrt{z_7^4 - 1}/(2z_7^2)$ . Thus,  $L_c$  increases as the boundary worldlines are oriented more along the  $x_1$  direction.

## Acknowledgments

We would like to thank Jacques Distler, Paul Esposito, Joshua Friess, Richard Gass, Steven Gubser, Andreas Karch, Juan Maldacena, Georgios Michalogiorgakis, Peter Moomaw, Leopoldo Pando Zayas, Silviu Pufu and John Wittig for helpful conversations. We are also indebted to Mariano Chernicoff, Antonio García, Alberto Güijosa, Hong Liu, Krishna Rajagopal, Kostas Sfetsos, and Urs Wiedemann for correspondence pointing out errors and shortcomings of an earlier version of this paper. We are grateful to the University of Michigan, the 2006 PITP school at the IAS, and the 4th Simons workshop at YITP for their hospitality. This research is supported by DOE grant FG02-84ER-40153.

## References

- [1] J.M. Maldacena, *The large  $N$  limit of superconformal field theories and supergravity*, Adv. Theor. Math. Phys. **2** (1998) 231; Int. J. Theor. Phys. **38** (1999) 1113, hep-th/9711200.

- [2] S.S. Gubser, I.R. Klebanov and A.M. Polyakov, *Gauge theory correlators from non-critical string theory*, Phys. Lett. B **428**, 105 (1998), hep-th/9802109.
- [3] E. Witten, *Anti-de Sitter space and holography*, Adv. Theor. Math. Phys. **2**, 253 (1998), hep-th/9802150.
- [4] O. Aharony, S.S. Gubser, J. Maldacena, H. Ooguri and Y. Oz, *Large  $N$  field theories, string theory and gravity*, Phys. Rept. **323** (2000) 183, hep-th/9905111.
- [5] A. Karch and E. Katz, *Adding flavor to AdS/CFT*, JHEP **0206** (2002) 043, hep-th/0205236.
- [6] P. Kovtun, D.T. Son and A.O. Starinets, *Holography and hydrodynamics: Diffusion on stretched horizons*, JHEP **10** (2003) 064, hep-th/0309213.
- [7] A. Buchel and J.T. Liu, *Universality of the shear viscosity in supergravity*, Phys. Rev. Lett. **93** (2004) 090602, hep-th/0311175.
- [8] P. Kovtun, D.T. Son and A.O. Starinets, *Viscosity in strongly interacting quantum field theories from black hole physics*, Phys. Rev. Lett. **94** (2005) 111601, hep-th/0405231.
- [9] A. Buchel, *On universality of stress-energy tensor correlation functions in supergravity*, Phys. Lett. **B609** (2005) 392, hep-th/0408095.
- [10] E. Shuryak, *Why does the quark gluon plasma at RHIC behave as a nearly ideal fluid?*, Prog. Part. Nucl. Phys. **53** (2004) 273, hep-ph/0312227.
- [11] E. Shuryak, *What RHIC experiments and theory tell us about properties of quark-gluon plasma?*, Nucl. Phys. **A750** (2005) 64, hep-ph/0405066.
- [12] R. Baier, D. Schiff and B.G. Zakharov, *Energy loss in perturbative QCD*, Ann. Rev. Nucl. Part. Sci. **50** (2000) 37, hep-ph/0002198.
- [13] A. Kovner and U.A. Wiedemann, *Gluon radiation and parton energy loss*, hep-ph/0304151.

- [14] M. Gyulassy, I. Vitev, X.N. Wang and B.W. Zhang, *Jet quenching and radiative energy loss in dense nuclear matter*, nucl-th/0302077.
- [15] P. Jacobs and X.N. Wang, *Matter in extremis: ultrarelativistic nuclear collisions at RHIC*, Prog. Part. Nucl. Phys. **54** (2005) 443, hep-ph/0405125.
- [16] H. Liu, K. Rajagopal and U.A. Wiedemann, *Calculating the jet quenching parameter from AdS/CFT*, Phys. Rev. Lett. **97** (2006) 182301, hep-ph/0605178.
- [17] C.P. Herzog, A. Karch, P. Kovtun, C. Kozcaz and L.G. Yaffe, *Energy loss of a heavy quark in  $N = 4$  super Yang-Mills plasma*, JHEP **0607** (2006) 013, hep-th/0605158.
- [18] S.S. Gubser, *Drag force in AdS/CFT*, hep-th/0605182.
- [19] C.P. Herzog, *Energy loss of heavy quarks from asymptotically AdS geometries*, JHEP **0609** (2006) 032, hep-th/0605191.
- [20] J. Casalderrey-Solana and D. Teaney, *Heavy quark diffusion in strongly coupled  $N = 4$  Yang Mills*, Phys. Rev. D **74** (2006) 085012, hep-ph/0605199.
- [21] A. Buchel, *On jet quenching parameters in strongly coupled non-conformal gauge theories*, Phys. Rev. D **74** (2006) 046006, hep-th/0605178.
- [22] C.P. Herzog, *Energy loss of heavy quarks from asymptotically AdS geometries*, JHEP **0609** (2006) 032, hep-th/0605191.
- [23] E. Caceres and A. Guijosa, *Drag force in charged  $N = 4$  SYM plasma*, JHEP **0611** (2006) 077, hep-th/0605235.
- [24] J.J. Friess, S.S. Gubser, G. Michalogiorgakis, *Dissipation from a heavy quark moving through  $N=4$  super-Yang-Mills plasma*, JHEP **0609** (2006) 072, hep-th/0605292.
- [25] J.F. Vázquez-Poritz, *Enhancing the jet quenching parameter from marginal deformations*, hep-th/0605296.

- [26] S.-J. Sin and I. Zahed, *Ampere's Law and energy loss in AdS/CFT duality*, hep-ph/0606049.
- [27] E. Caceres and A. Guijosa, *On drag forces and jet quenching in strongly coupled plasmas*, hep-th/0606134.
- [28] F.-L. Lin and T. Matsuo, *Jet quenching parameter in medium with chemical potential from AdS/CFT*, Phys. Lett. B **641** (2006) 45, hep-th/0606136.
- [29] S.D. Avramis and K. Sfetsos, *Supergravity and the jet quenching parameter in the presence of R-charge densities*, hep-th/0606190.
- [30] K. Peeters, J. Sonnenschein and M. Zamaklar, *Holographic melting and related properties of mesons in a quark gluon plasma*, Phys. Rev. D **74** (2006) 106008, hep-th/0606195.
- [31] N. Armesto, J.D. Edelstein and J. Mas, *Jet quenching at finite 't Hooft coupling and chemical potential from AdS/CFT*, JHEP **0609** (2006) 039, hep-ph/0606245.
- [32] Y.h. Gao, W.S. Xu and D.F. Zeng, *Wake of color fields in charged  $N = 4$  SYM plasmas*, hep-th/0606266.
- [33] J.J. Friess, S.S. Gubser, G. Michalogiorgakis and S.S. Pufu, *The stress tensor of a quark moving through  $N = 4$  thermal plasma*, hep-th/0607022.
- [34] H. Liu, K. Rajagopal and U.A. Wiedemann, *An AdS/CFT calculation of screening in a hot wind*, hep-ph/0607062.
- [35] M. Chernicoff, J. Antonio Garcia and A. Guijosa, *The energy of a moving quark-antiquark pair in an  $\mathcal{N} = 4$  SYM plasma*, JHEP **0609** (2006) 068, hep-th/0607089.
- [36] T. Matsuo, D. Tomino and W.-Y. Wen, *Drag force in SYM plasma with B field from AdS/CFT*, JHEP **0610** (2006) 055, hep-th/0607178.
- [37] E. Caceres, M. Natsuume and T. Okamura, *Screening length in plasma winds*, JHEP **0610** (2006) 011, hep-th/0607233.

- [38] S. Rey and J. Yee, *Macroscopic strings as heavy quarks in large  $N$  gauge theory and anti-de Sitter supergravity*, Eur. Phys. J. **C22** (2001) 379, hep-th/9803001.
- [39] J.M. Maldacena, *Wilson loops in large  $N$  field theories*, Phys. Rev. Lett. **80** (1998) 4859, hep-th/9803002.
- [40] S.J. Rey, S. Theisen and J.T. Yee, *Wilson-Polyakov loop at finite temperature in large  $N$  gauge theory and anti-de Sitter supergravity*, Nucl. Phys. **B527** (1998) 171, hep-th/9803135.
- [41] A. Brandhuber, N. Itzhaki, J. Sonnenschein and S. Yankielowicz, *Wilson loops in the large  $N$  limit at finite temperature*, Phys. Lett. **B434** (1998) 36, hep-th/9803137.
- [42] S.D. Avramis, K. Sfetsos and D. Zoakos, *On the velocity and chemical-potential dependence of the heavy-quark interaction in  $N = 4$  SYM plasmas*, hep-th/0609079.
- [43] J.J. Friess, S.S. Gubser, G. Michalogiorgakis and S.S. Pufu, *Stability of strings binding heavy-quark mesons*, hep-th/0609137.
- [44] P. Argyres, M. Edalati and J.F. Vázquez-Poritz, *Spacelike strings and jet quenching from a Wilson loop*, hep-th/0612157.
- [45] J. Babington, J. Erdmenger, N.J. Evans, Z. Guralnik and I. Kirsch, *Chiral symmetry breaking and pions in non-supersymmetric gauge/gravity duals*, Phys. Rev. D **69**, 066007 (2004), hep-th/0306018.
- [46] D. Mateos, R.C. Myers and R.M. Thomson, *Holographic phase transitions with fundamental matter*, Phys. Rev. Lett. **97** (2006) 091601, hep-th/0605046.
- [47] A. Karch and A. O'Bannon, *Chiral transition of  $N = 4$  super Yang-Mills with flavor on a 3-sphere*, Phys. Rev. D **74** (2006) 085033, hep-th/0605120.
- [48] T. Albash, V. Filev, C.V. Johnson and A. Kundu, *A topology-changing phase transition and the dynamics of flavour*, hep-th/0605088.

- [49] T. Albash, V. Filev, C.V. Johnson and A. Kundu, *Global currents, phase transitions, and chiral symmetry breaking in large  $N(c)$  gauge theory*, hep-th/0605175.